NASA
Technical Memorandum 82865

AVRADCOM
Technical Report 82-C-8

A Finite Element Stress Analysis of Spur Gears Including Fillet Radii and Rim Thickness Effects

S. H. Chang and R. L. Huston
University of Cincinnati
Cincinnati, Ohio

and

J. J. Coy
Propulsion Laboratory
AVRADCOM Research and Technology Laboratories
Lewis Research Center
Cleveland, Ohio

Prepared for the
Winter Annual Meeting of the
American Society of Mechanical Engineers
Phoenix, Arizona, November 14-19, 1982

NASA

U.S. ARMY AVRADCOM

A FINITE ELEMENT STRESS ANALYSIS OF SPUR GEARS INCLUDING FILLET RADII AND RIM THICKNESS EFFECTS

S. H. Chang and R. L. Huston
Department of Mechanical Engineering
University of Cincinnati
Cincinnati, Ohio 45221

and

J. J. Coy
Propulsion Laboratory
AVRADCOM Research and Technology Laboratory
NASA Lewis Research Center
Cleveland, Ohio 44135

E-1234

ABSTRACT

Spur gear stress analysis results are presented for a variety of loading conditions, support conditions, fillet radii, and rim thicknesses. These results are obtained using the SAP IV finite-element code. The maximum stresses, occurring at the root surface, substantially increase with decreasing rim thickness for partially supported rims (that is, with loose-fitting hubs). For fully supported rims (that is, with tight-fitting hubs), the root surface stresses slightly decrease with decreasing rim thickness. The fillet radius is found to have a significant effect upon the maximum stresses at the root surface. These stresses increase with decreasing fillet radius. The fillet radius has little effect upon the internal root section stresses.

INTRODUCTION

During the past decade there have been a number of investigations into the nature of spur gear stresses. References [1-12]* summarize some of these efforts. They include a variety of theoretical and experimental approaches to determining the stresses, but the results are reasonably consistent. Of particular interest is the fact that the results obtained using finite element techniques are consistent with results obtained using vastly different theoretical and experimental techniques. For example, in 1955, Jacobson [13] studied bending stresses using photoelastic techniques. In 1973, his results were matched by Wilcox and Coleman [11] using finite element techniques. In 1962, Aida and Terauchi [14] studied bending stresses using stress functions and classical elasticity theories, and more recently (1981) Cordou and Tordion [2] studied the stresses using complex variables. Their results also confirm results obtained using finite element techniques. Other noteworthy theoretical studies which confirm finite element results are those of Baronet, Tordion, and Premilhat [1,7] and of Shotter [8].

Regarding the use of the finite element method itself in gear stress analyses, there have recently been a number of notable achievements. For

*Numbers in brackets refer to References at the end of the paper.

example, Chabert, Dang Tran, and Mathis [3] have used finite element techniques to examine the stress distribution across the root section. Tobe, Kato and Inoue [9,10], Winter and Hirt [12], Cornell [5], and Wilcox and Coleman [11] have studied root stresses using finite element methods. Finally, Oda, Nagamura, and Aoki have examined the effect of rim thickness on the root stresses using the finite element method.

In view of this, the objectives of the research effort of this paper are to determine (a) the surface stress distribution for the entire tooth profile for tip and pitch point loading; (b) the fillet stresses and the root section stresses for a variety of loading positions and fillet radii; and (c) the effect of rim thickness and mounting support upon the root stress. The SAP IV finite element technique [15] was used in the analysis.

ANALYSIS

The Model

Figure 1 shows typical finite-element grids used in the analysis. The number of elements used was varied depending upon the particular loading and geometry being considered. Typically the grid had approximately 190 elements and 120 nodes.

The gear tooth itself had a modulus M of 5 (pitch diameter divided by the number of teeth). It was a member of an 18-tooth gear with the pitch diameter thus being 90 mm. The tooth sides are involute curves and the pressure angle was 20°. The fillet radius and hub thickness were variables. The tooth material was steel with an elastic modulus of 2.11×10^5 N/mm^2.

Loading and Support

The tooth was loaded with a 400 N/mm concentrated line load applied normal to the tooth boundary at various points as shown in Figure 2. The hub or rim was supported alternatively: a) at all points along the boundary, and b) at only the radial points.

The Finite Element Procedure

The SAP IV technique [15] was used to assemble and solve the governing equations

$$Ku = R \tag{1}$$

where K is the global stiffness matrix, u is the array of nodal displacements and R is the force array. The solution is obtained using Gauss elimination through the linear equation solver SESOL [15]. After the nodal displacements are found, element stress displacement relations are used to obtain the element stresses.

RESULTS

Surface Stress Distribution

First, the stress distribution along the tooth surface was calculated for a tip loading and for a load applied near the pitch point. Figure 3 contains

a representation of the results for the maximum principal surface stress. They show that, except for a local concentration, the maximum stress occurs at the root of the tooth.

Root Surface Stresses as a Function of the Root Radius

The above analysis led to a closer examination of the maximum fillet stresses as a function of the fillet radius. Specifically, the tooth was loaded at the points shown in Figure 2. The fillet stresses were then calculated for radii of 0.2M, 0.3M, and 0.4M or 1.0 mm, 1.5 mm, and 2.0 mm, respectively. The results for the 1.0 mm and 2.0 mm fillet radii are shown in Figure 2. The results for the 1.5 mm fillet radii are intermediate to these. An examination of the numerical values associated with these results shows the stresses increase linearly with the inverse of the fillet radii, for the range of radii considered. Also, the stresses are seen to increase linearly with the distance from the fillet to the point of application of the load. These results are consistent with those obtained and recorded by Chabert, et al. [3], and with those of short beam theory as recorded by Roark and Young [16].

Internal Root Section Stresses as a Function of Root Radius and Loading Position

Figures 4 and 5 show the principal stress distribution across the root section for tip loading and for pitch point loading for the various fillet radii. As expected, the stresses are smallest at the center of the section and the largest stresses occur at the surface. Interestingly, the fillet radius has little effect upon the internal stress distribution.

Effect of Rim Thickness and Support Conditions

Figures 6 to 10 show the effect of the rim thickness and the hub or rim support upon the fillet stresses and the stresses across the root section. Specifically, Figure 6 shows the surface stresses for a gear tooth with a fully supported rim (that is, supported at the rim base and along the radial sides, simulating tight fitting hubs). The fillet radius was 2.0 mm and the rim radii were 35.0 mm and 37.1 mm. The loading was the same as that shown in Figure 3.

Similarly, Figure 7 shows the fillet stresses for a gear tooth with a partially supported rim (that is, supported only along the radial sides, simulating loose fitting hubs). The fillet radii, rim radii and loading were the same as with the fully supported rim.

These results show that when the rim is fully supported the fillet stresses decrease slightly as the rim thickness decreases. However, when the rim is only partially supported the fillet stresses increase substantially as the rim thickness decreases. Moreover, for partially supported rims the compressive stresses, at the fillet opposite the loaded side increase at a greater rate than the tensile stresses at the fillet of the loaded side. These results are summarized graphically in Figure 8.

Finally, figures 9a and 10a show the internal root section principal stresses for a fully supported rim with the same root radii and rim radii as above. The loading was at the tip as shown with a magnitude of 400 N/mm as

before. Similarly, Figures 9b and 10b show the internal root section principal stresses for a partially supported rim with the same fillet radii, rim radii, and loading. These results also show that the stresses decrease slightly with decreasing rim thickness for fully supported rims, but they increase with rim thickness for partially supported rims.

These results are consistent with recent experimental findings recorded by Drago and Lutthans [17].

SUMMARY

1. The rim thickness and rim support have a significant effect upon the stresses - particularly for partially supported thin rims, with the compressive root stresses, opposite the loading side, being most affected. The stresses increase with decreasing rim thickness for partially supported rims (such as with loose-fitting hubs). However, for fully supported rims (such as with tight-fitting hubs) the stresses decrease slightly with decreasing rim thickness. For large rim thickness the rim support has little effect upon the stresses.

2. The maximum stresses occur at the root surfaces, except for local stress concentrations immediately beneath the load. These root stresses increase with decreasing fillet radii.

3. The fillet radius has very little effect upon the internal root section stresses.

4. The SAP IV finite-element method is a very effective procedure for investigating gear tooth stresses with a variety of loading, support, and geometrical shapes. This method can provide a benchmark analysis of gear tooth stresses, replacing many of the currently used handbook formulae.

REFERENCES

1. Baronet, C. N., and Tordion, G. V., "Exact Stress Distribution in Standard Gear Teeth and Geometry FActors," ASME Journal of Engineering for Industry, Vol. 95, No. 4, Nov. 1973, pp. 1159-1163.

2. Cardou, A., and Tordion, G. V., "Numerical Implementation of Complex Potentials for Gear Tooth Stress Analysis," ASME Journal of Mechanical Design, Vol. 103, No. 2, Apr. 1981, pp. 461-465.

3. Chabert, G., Dang Tran, T., and Mathis, R., "An Evaluation of Stresses and Deflection of Spur Gear Teeth Under Strain," ASME Journal of Engineering for Industry, Vol. 96, No. 1, Feb. 1974, pp. 85-93.

4. Chan, S. K., and Tuba, I. S., "A Finite Element Method for Contact Problems of Solid Bodies - Part 1. Theory and Validation," International Journal of Mechanical Sciences, Vol. 13, No. 7, Apr. 1971, pp. 615-625.

5. Cornell, R. W., "Compliance and Stress Sensitivity of Spur Gear Teeth," ASME Journal of Mechanical Design, Vol. 103, No. 2, Apr. 1981, pp. 447-459.

6. Oda, S., Nagamura, K., and Aoki, K., "Stress Analysis of Thin Rim Spur Gears by Finite Element Method," Bulletin of the Japanese Society of Mechanical Engineers, Vol. 24, No. 193, July 1981, pp. 1273-1280.

7. Premilhat, A., Tordion, G. V., and Baronet, C. N., "An Improved Determination of the Elastic Compliance of a Spur Gear Tooth Acted on by a Concentrated Load," ASME Journal of Engineering for Industry, Vol. 96, No. 2, May 1974, pp. 382-384.

8. Shotter, B. A., "A New Approach to Gear Tooth Root Stresses," ASME Journal of Engineering for Industry, Vol. 96, No. 1, Feb. 1974, pp. 11-18.

9. Tobe, T., Kato, M., and Inoue, K., "Bending of Stub Cantilever Plate and Some Applications to Strength of Gear Teeth," ASME Journal of Mechanical Design, Vol. 100, No. 2, Apr. 1978, pp. 374-381.

10. Tobe, T., Kato, M., and Inoue, K., "True Stress and Stiffness of Spur Gear Teeth," Proceedings of the Fifth World Conference on Theory of Machines and Mechanisms, ASME, 1979, pp. 1105-1108.

11. Wilcox, L., and Coleman, W., "Application of Finite Elements to the Analysis of Gear Tooth Stresses," ASME Journal of Engineering for Industry, Vol. 95, No. 4, Nov. 1973, pp. 1139-1148.

12. Winter, H., and Hirt, M., "The Measurement of Actual Strains at Gear Teeth, Influence of Fillet Radius on Stresses and Tooth Strength," ASME Journal of Engineering for Industry, Vol. 96, No. 1, Feb. 1974, pp. 33-50.

13. Jacobson, M. A., "Bending Stresses in Spur Gear Teeth: Proposed New Design Factors Based on a Photo-Elastic Investigation," Proceedings, Institution of Mechanical Engineers, Vol. 169, 1955, pp. 587-609.

14. Aida, T., and Terauchi, Y., "On the Bending Stress of a Spur Gear, Bulletin of the Japanese Society of Mechanical Engineers, Vol. 5, No. 17, Feb. 1962, pp. 161-170.

15. Bathe, K. J., Wilson, E. L., and Peterson, F. E., "SAP-IV - A Structural Analysis Program for Static and Dynamic Response of Linear Systems," Report No. EERC 73-11, Earthquake Engineering Research Center, University of California, Berkeley, CA, 1974.

16. Roark, R. J., and Young, W. C., Formulas for Stress and Strain, 5th ed. McGraw-Hill, New York, 1975, p. 187.

17. Drago, R. J., and Lutthans, R. V., "An Experimental Investigation of the Combined Effects of Rim Thickness and Pitch Diameter on Spur Gear Tooth Root and Fillet Stresses," AGMA Paper No. P229.22, American Gear Manufacturers Association Fall Technical Meeting, Toronto, 1981.

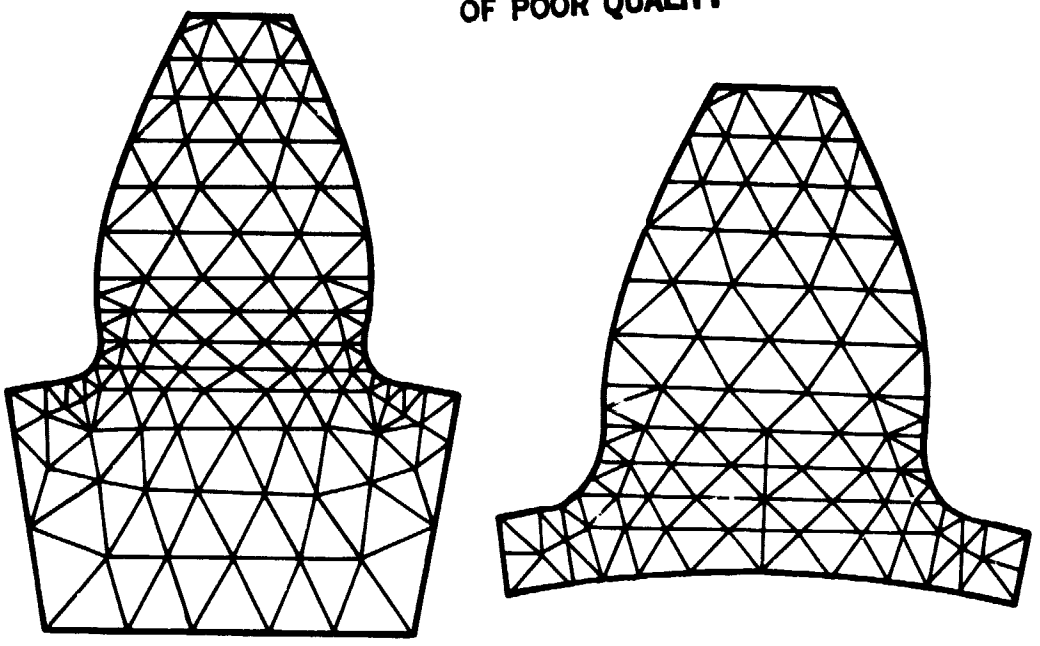

(a) Small fillet radius. (b) Small rim thickness.

Figure 1. - Typical finite element grids.

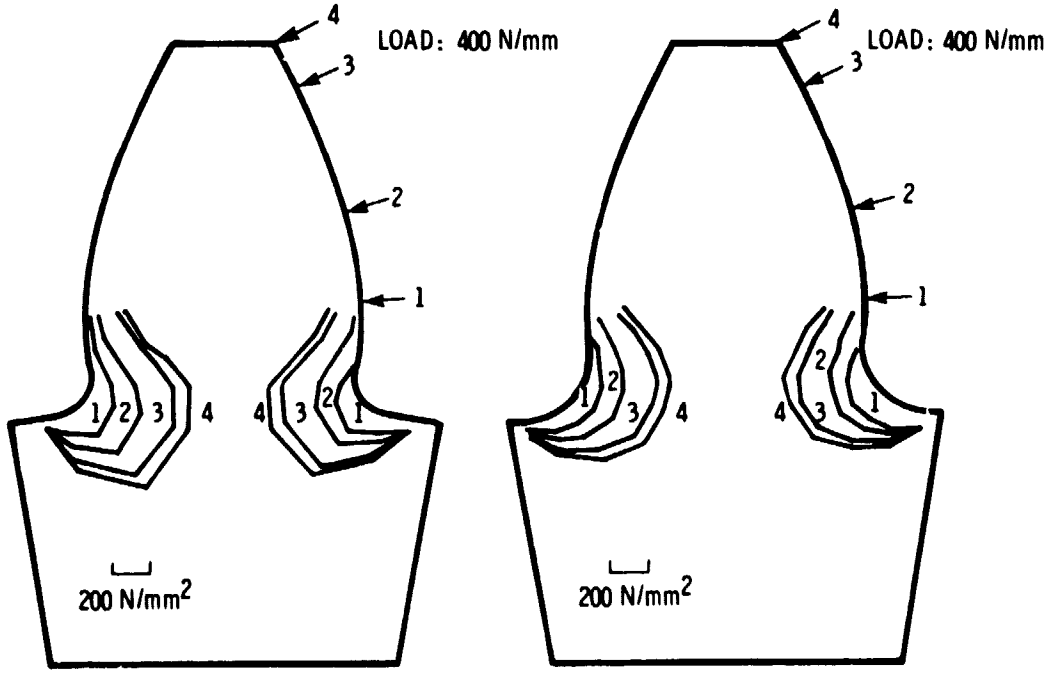

(a) 1.0 mm fillet radius. (b) 2.0 mm radius.

Figure 2. - Surface stress distribution at the fillet.

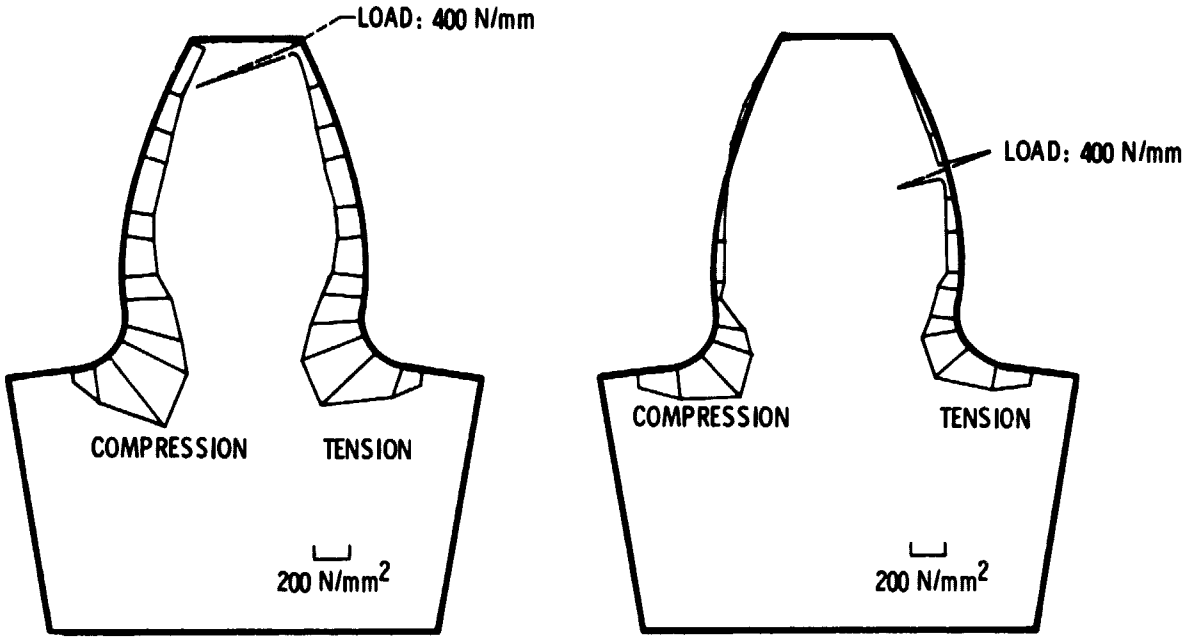

(a) Tip loading. (b) Pitch point loading.

Figure 3. - Surface maximum stress distribution.

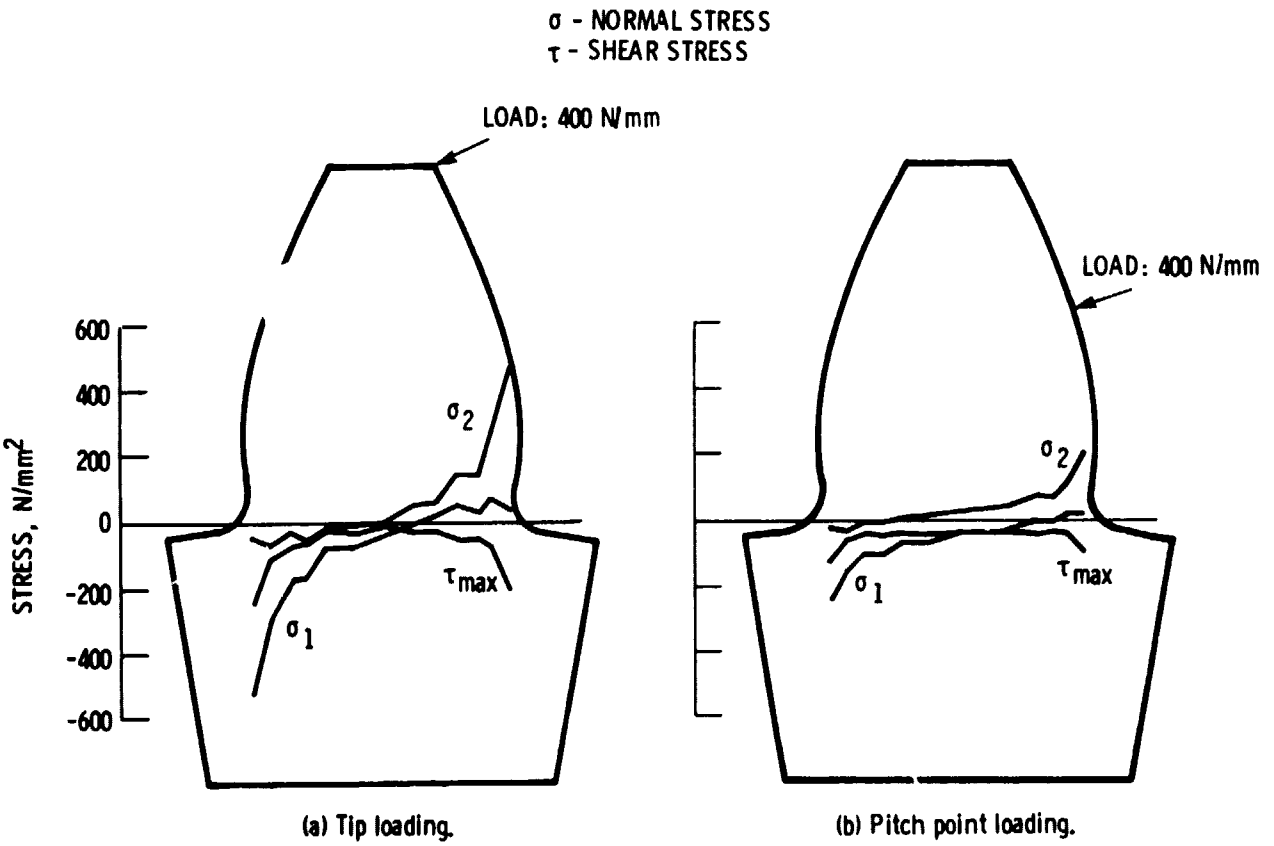

(a) Tip loading. (b) Pitch point loading.

Figure 4. - Internal root section principal stresses for 1.0 mm fillet radius.

σ - NORMAL STRESS
τ - SHEAR STRESS

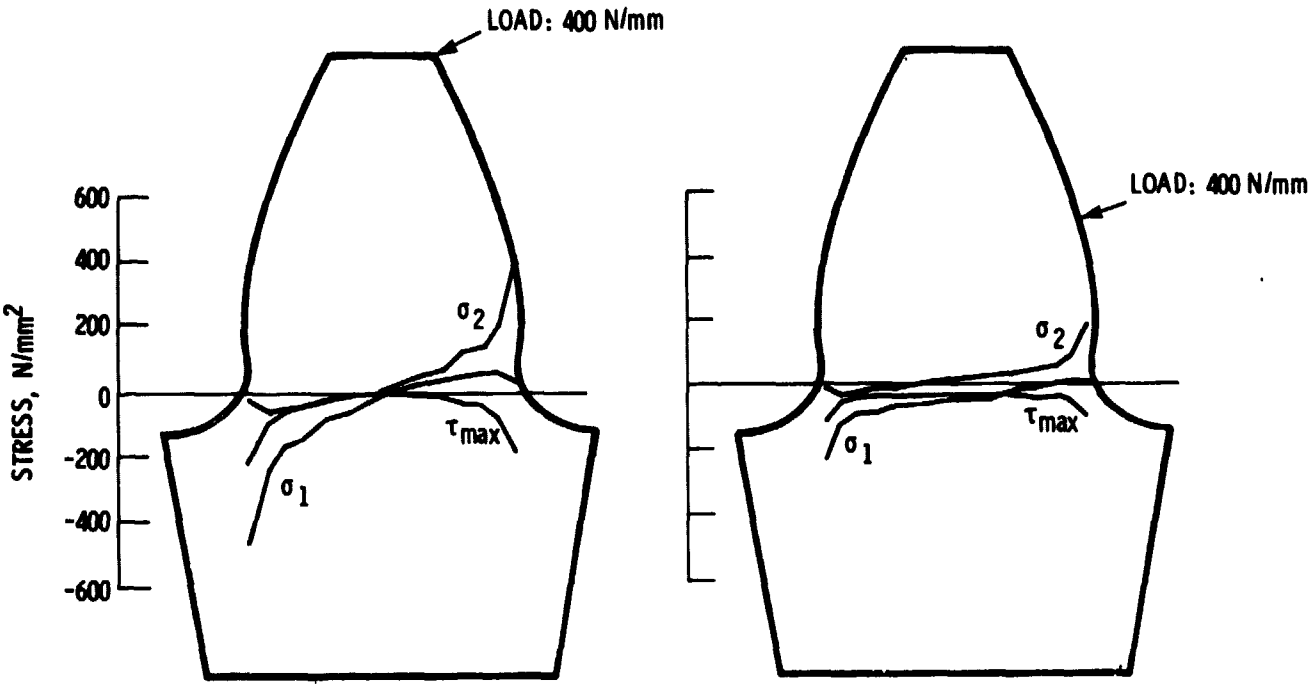

(a) Tip loading

(b) Pitch point loading.

Figure 5. - Internal root section principal stresses for 2.0mm fillet radius.

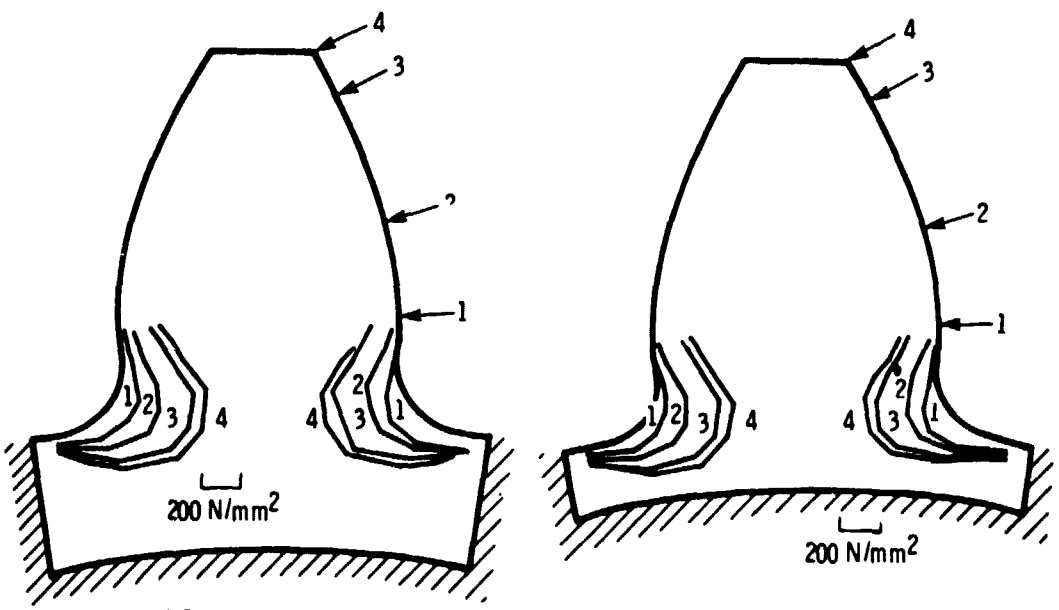

(a) Rim radius: 35mm.

(b) Rim radius: 37.1 mm.

Figure 6. - Surface stress distribution at the fillet for a fully supported rim.

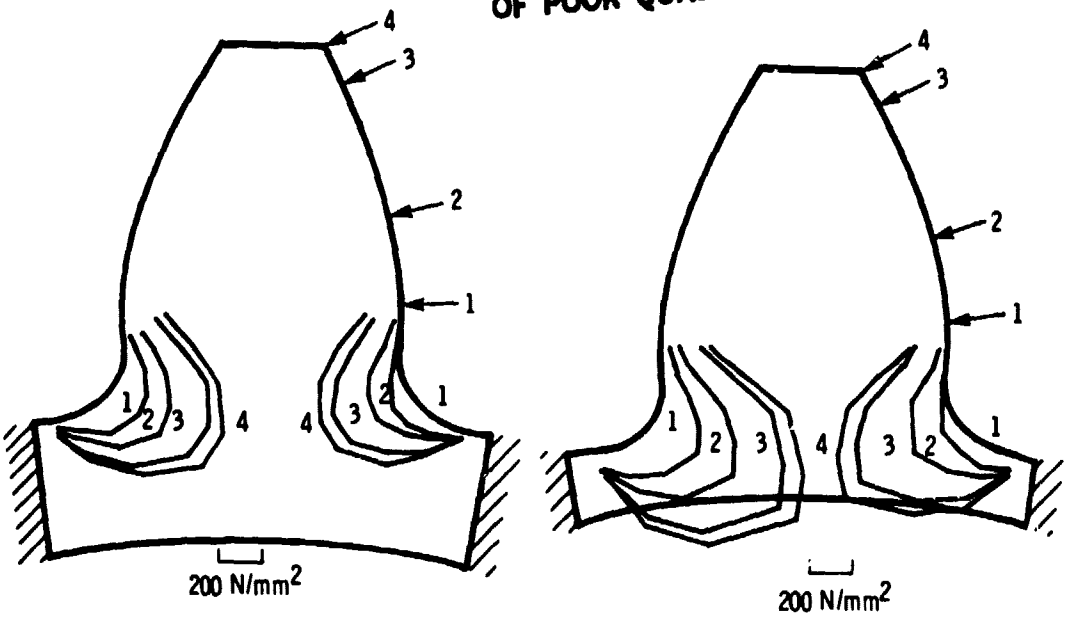

(a) Rim radius: 35mm.

(b) Rim radius: 37. 1mm.

Figure 7. - Surface stress distribution at the fillet for a partially supported rim.

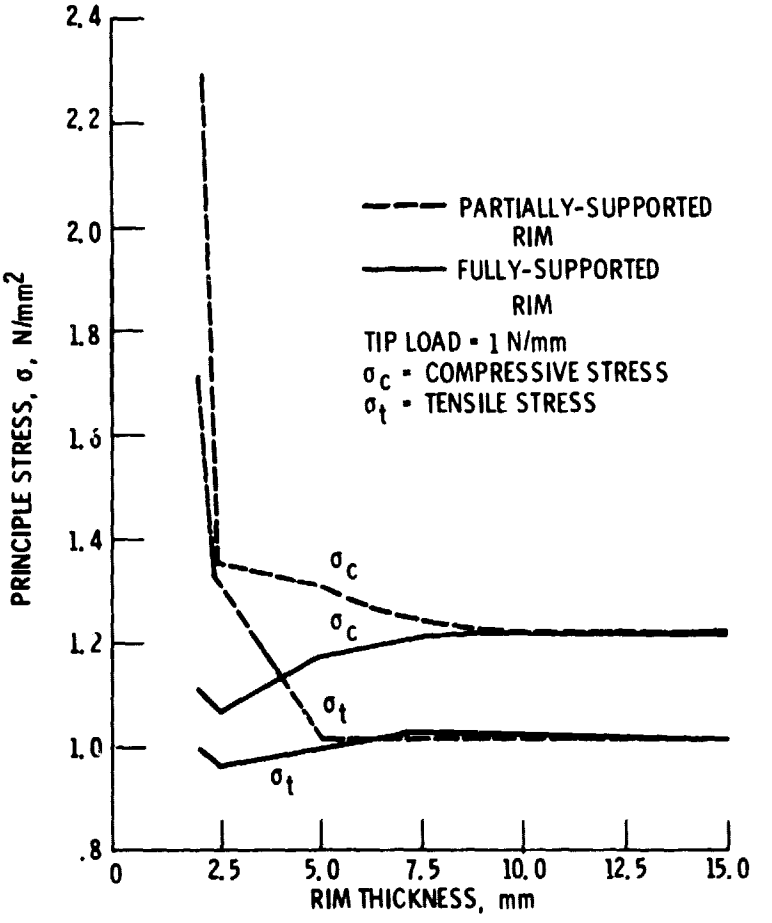

Figure 8. - Variation of maximum fillet stresses with rim thickness.

σ - NORMAL STRESS
τ - SHEAR STRESS

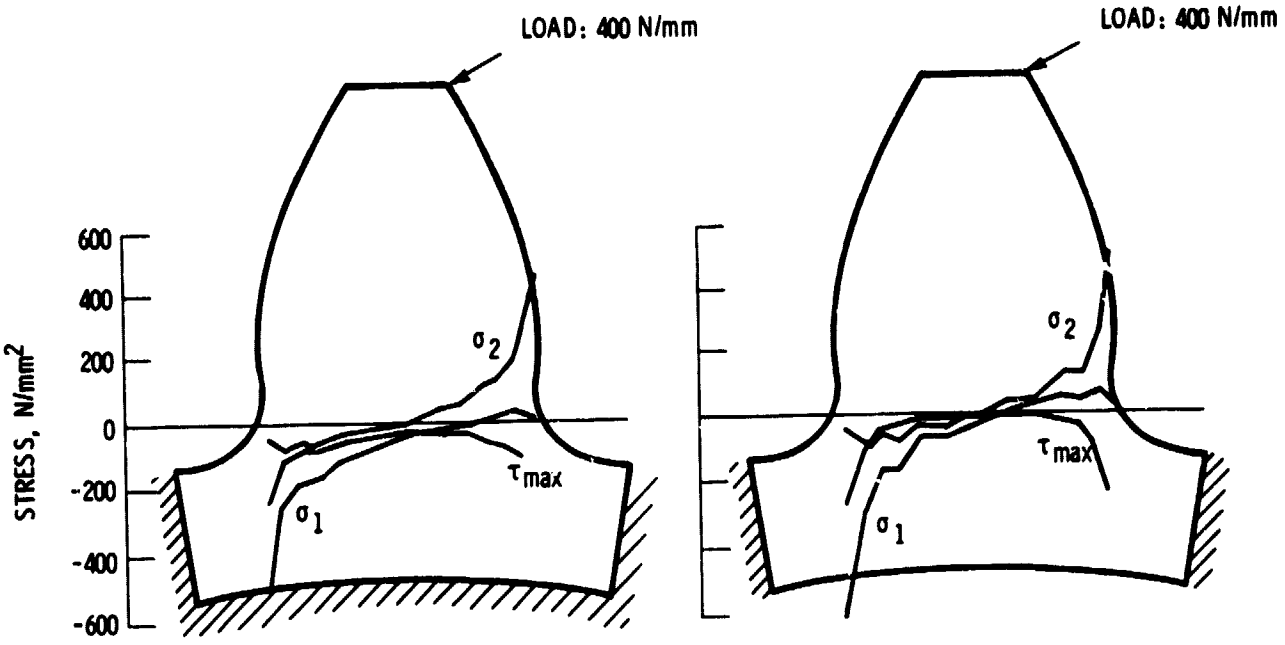

(a) Fully supported rim.

(b) Partially supported rim.

Figure 9. - Internal root section principal stresses with tip loading with a rim radius of 35mm.

σ - NORMAL STRESS
τ - SHEAR STRESS

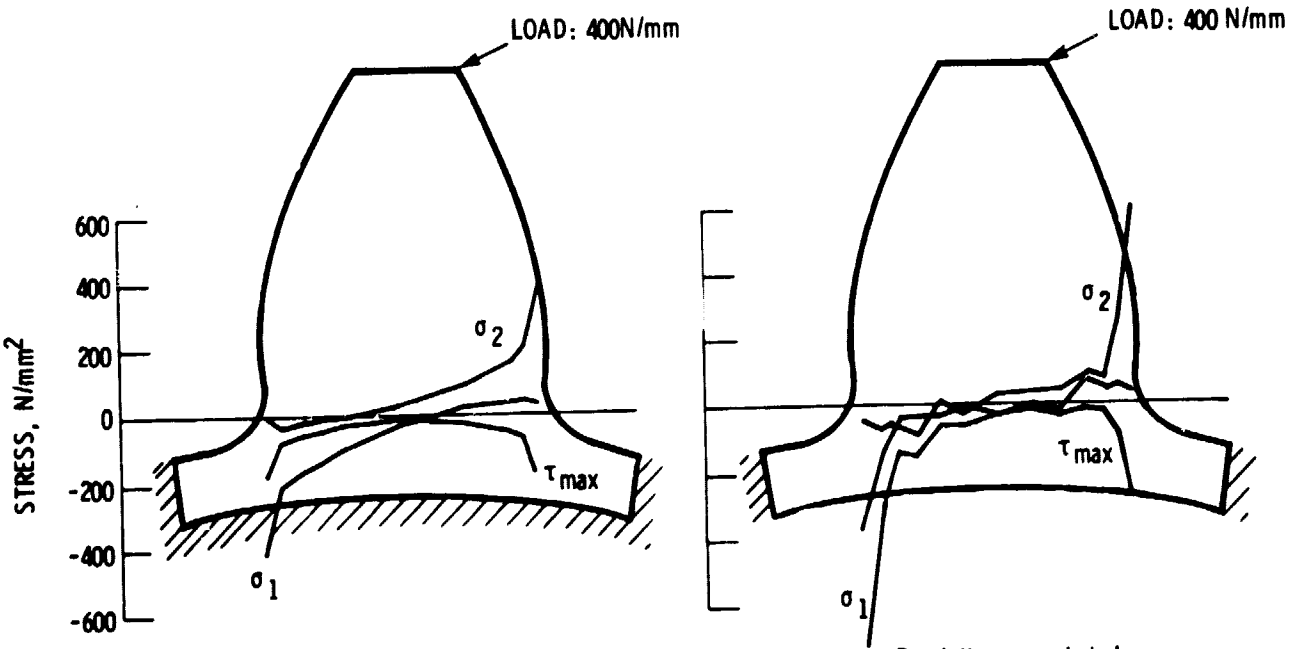

(a) Fully supported rim.

(b) Partially supported rim.

Figure 10. - Internal root section principal stresses with tip loading with a rim radius of 37.1mm.